Schlussbericht, 27. März 2003

Turbulente chemisch reactive Strömung in Motorbrennräumen

Autor und Koautoren	Dr. Christos E. Frouzakis, Prof. Dr. Konstantinos Boulouchos
beauftragte Institution	Laboratory of Aerothermochemistry and combustion systems LAV
Adresse	Institute of Energy Technology, IET ETH Zentrum Clausiusstrasse 33 CH-8092 Zürich
Telefon, E-mail, Internetadresse	01-632 79 47, frouzakis@lav.mavt.ethz.ch, www.lav.ethz.ch
BFE Projekt-/Vertrag-Nummer	35154
Dauer des Projekts (von – bis)	1.4.1999 – 31.3.2002

Zusammenfassung

Das Ziel des vorliegenden Projektes war, das Werkzeug der Direkten Numerischen Simulation zum vertieften Verständnis von generischen Fällen der Wechselwirkung zwischen Turbulenz und chemischer Kinetik einzusetzen und durch Weiterentwicklung des entesprechenden Code Wege aufzuzeigen, wie erste Berechnungen für Flammen von technischer Bedeutung (in Anwendungen) in der nahen Zukunft modellfrei durchgeführt werden können.

Beide Ziele wurden praktisch vollständig erreicht. Als Beispiele für die Beschreibung von komplexen Interaktionen zwischen Strömungsparameterern und laminaren Flammen, erwähnen wir in diesem Bericht einerseits die detaillierte Untersuchung des Übergangs von gestrechten Diffusions- zu vorgemischten „edge flames“ und vice-versa und anderseits instationäre Effekte (Löschen und Widerzünden) von Diffusionsflammen am Gegenstrombrenner. Beide Fälle, welche als sehr wesentlich für das Verständnis und die Modellierung der turbulenten Verbrennung erachtet werden, sind erstmals in diesem Umfang studiert und die entsprechenden Arbeiten an renommierten Journals veröffentlicht.

Inzwischen ist der ursprüngliche 2-D Code –in Zusammenarbeit mit dem Argonne National Lab- soweit entwickelt worden, dass eine voll parallelisierte 3-D Version für komplexe Geometrien mit „Ein-Schritt“-Reaktionskinetik praktisch fertiggestellt ist. Damit und mit Hilfe des neu an unserem Laboratorium anzuschaffenden PC-Linux-Cluster werden wir in der nahe Zukunft in der Lage sein, erste DNS-Simulationen für Flammen bei turbulenten oder Übergangsströmung durchzuführen.

BFE OFEN UFE SFOE

1 Project description

Direct Numerical Simulation (DNS) is a powerful tool to study in detail combustion phenomena. It solves the system of governing equations with high spatial and temporal accuracy and can provide information that cannot be obtained by other means. Unfortunately, it also carries a very high computational cost, rendering it impractical for practical combustion applications. Nevertheless, the in-depth understanding of the physico-chemical processes that can be provided by the analysis of DNS results can be used to validate or better understand the limitations of models currently used in turbulent combustion codes and guide their improvement. The aim of this project is to use Direct Numerical Simulation to study phenomena of fundamental interest in laminar reactive flows that are also of importance under turbulent conditions.

2 Numerical approach

Our simulation tool is based on the spectral element discretization of the partial differential equations describing the conservation equation of mass, momentum, species, and energy for two-dimensional chemically reacting system at the low Mach number limit. The spectral element method combines the flexibility of the finite element method to discretize complex geometries with the accuracy of spectral methods. A high-order stiffly-stable splitting scheme that separates the "hydrodynamic" (i.e. mass and momentum equations) from the "thermo-chemistry" (i.e. the species and energy equation) subsystems is used for time integration. The former is integrated using a high-order semi-implicit splitting procedure, leading to minimal errors in mass conservation, and to a decoupled solution procedure for the flow equations. A pressure Poisson equation, similar to that in incompressible flow, is derived for the "hydrodynamic pressure", accounting for the non-zero divergence of the velocity field. The species and energy equations are integrated without further splitting fully implicitly with a backward differentiation formula (BDF) based integrator. The overall high-order convergence rate of the algorithm has been verified using combined analytical asymptotic and numerical techniques. The formulation maintains its accuracy, demonstrated to be overall up to third order in time and spectral in space, for general geometries, typical of experimental combustion configurations and practical combustion devices [1, 2]. The code is coupled with the CHEMKIN library, and can easily handle both simplified and detailed chemistry and transport.

3 Main results

During the course of this project, the code performance was further improved, mainly by the use of more efficient time integrators for the stiff thermo-chemistry

part. The coupling with the VODPK BDF-based package [3], resulted in large savings in both memory and computational time. This version was then used for the simulation of (a) diffusion flame-vortex interactions, and (b) diffusion/edge flame transitions in hydrogen/air flames in the opposed-jet geometry using detailed chemistry and transport. The results of (a) were presented at the 17^{th} International Colloquium on the Dynamics of Explosions and Reactive Systems, and were published in Combustion Science and Technology [4]. The results from (b) were presented at the the 28^{th} and 29^{th} Symposia on Combustion and published in Combustion and Flame [5]. We have also used the Proper Orthogonal Decomposition (POD) technique for the reduction of the data obtained in our simulations as a first step towards the construction of low dimensional models for diffusion flames. It was also shown that the POD modes can be used to obtain observers of unknown quantities from partial information. These results where presented at the 28^{th} Symposium on Combustion.

3.1 Diffusion flame/vortex interactions

The flamelet model views a turbulent diffusion flame as an ensemble of laminar diffusion flamelets [6], which are stretched and distorted by vortices of different sizes and velocities created by the turbulent flow. Laminar diffusion flamelets can be pre-computed using detailed chemistry in one-dimensional opposed-jet setups and tabulated with respect to mixture fraction and scalar dissipation rate. The tables can then provide detailed chemistry information within CFD calculations, where the mixture fraction is solved for and the local scalar dissipation rate is obtained from the computed velocity field. The study of the interaction of laminar diffusion flames with vortices is therefore important in terms of fundamental understanding of turbulent flames, and are studied extensively experimentally as well as computationally.

We investigated the response of a flat N_2-diluted H_2/air diffusion flame stabilized on an opposed-jet burner to vortices of different sizes and velocities. The vortex is the so-called Hills vortex, described by an analytical expression in terms of its streamfunction and two parameters: its radius, a, and its strength, U_{Hills}. Our simulations demonstrated the opposite effects produced by flame curvature of different sign by placing the vortex on either the air or the fuel side of the diffusion flame. When the flame curvature is convex towards the fuel stream, the flame burns more intensely. On the other hand, if the flame curvature is convex towards the air stream, the flame weakens and, if the initial vortex is strong enough, extinguishes locally. Five cases with vortices of different initial size and strength, placed on either side of the flame were studied (a total of ten simulations). The detailed analysis of the simulations can be found in [4]. Here we only present a set of two simulations with a vortex of initial radius equal to the diffusion flame thickness. The time sequence showing variations in temperature and OH mass fraction (with the streamlines superimposed) is shown in Fig.

1. To illustrate the extinction, mixing, and reignition processes, we also plot the isocontours of the mass fractions of O_2 and H_2. Observations made from Fig. 1 can be summarized as follows:

- The diffusion flame extinguishes in a region centered on the axis of symmetry when the vortex is placed on the oxidizer side; temperature there dropped to almost 400K.
- The same vortex placed on the fuel size not only does not extinguish the flame, but it makes it burn more intensely.
- In both cases, it took approximately 120 ms for the flame to return to the steady-state.
- During relaxation, in the case of the vortex placed on the air side, the flame thickens considerably, and the temperature rises above the steady-state value of 1640K by almost 400K.

By extracting from our simulations the profiles along the axis of symmetry and using the one-dimensional code OPPDIF, we also compare the transient response of the diffusion flame with that of a steady-state flamelet. Fig. 2 demonstrates clearly transient effects as well as the effects of flame curvature, and differential diffusion on the response of the flame. It also shows that the extinction strain rate is dependent upon flame curvature. The latter can have a strong effect on the modeling of local extinction in flamelet models.

3.2 Diffusion/edge flame transitions

3.2.1 Steady results

In opposed-jet diffusion flame experiments, under certain conditions, after the extinction of the diffusion flame, an edge flame can be obtained. This ring-shaped edge flame has been reported first in 1959 by Potter *et al.* [7], but has since received little attention. It has been reported again recently in the experimental work of Pellet *et al.* [8] and is responsible for an interesting transition between two distinct vigorously burning flames (multiple solutions). Motivated by our previous numerical results obtained with simplified kinetics [1] and the experimental data of Pellet *et al.* [8], we performed numerical simulations of this transition to investigate the underlying physical mechanisms [9]. The appearance of an edge flame after the extinction of the diffusion flame, the hysteresis reported in the experiments, and the existence of multiple vigorously burning flames at identical conditions were all captured by our simulations. Our numerical results show that, in the absence of the inert co-flow curtain, when the diffusion flame disk is extinguished, an edge flame can form and propagate in the mixing layer.

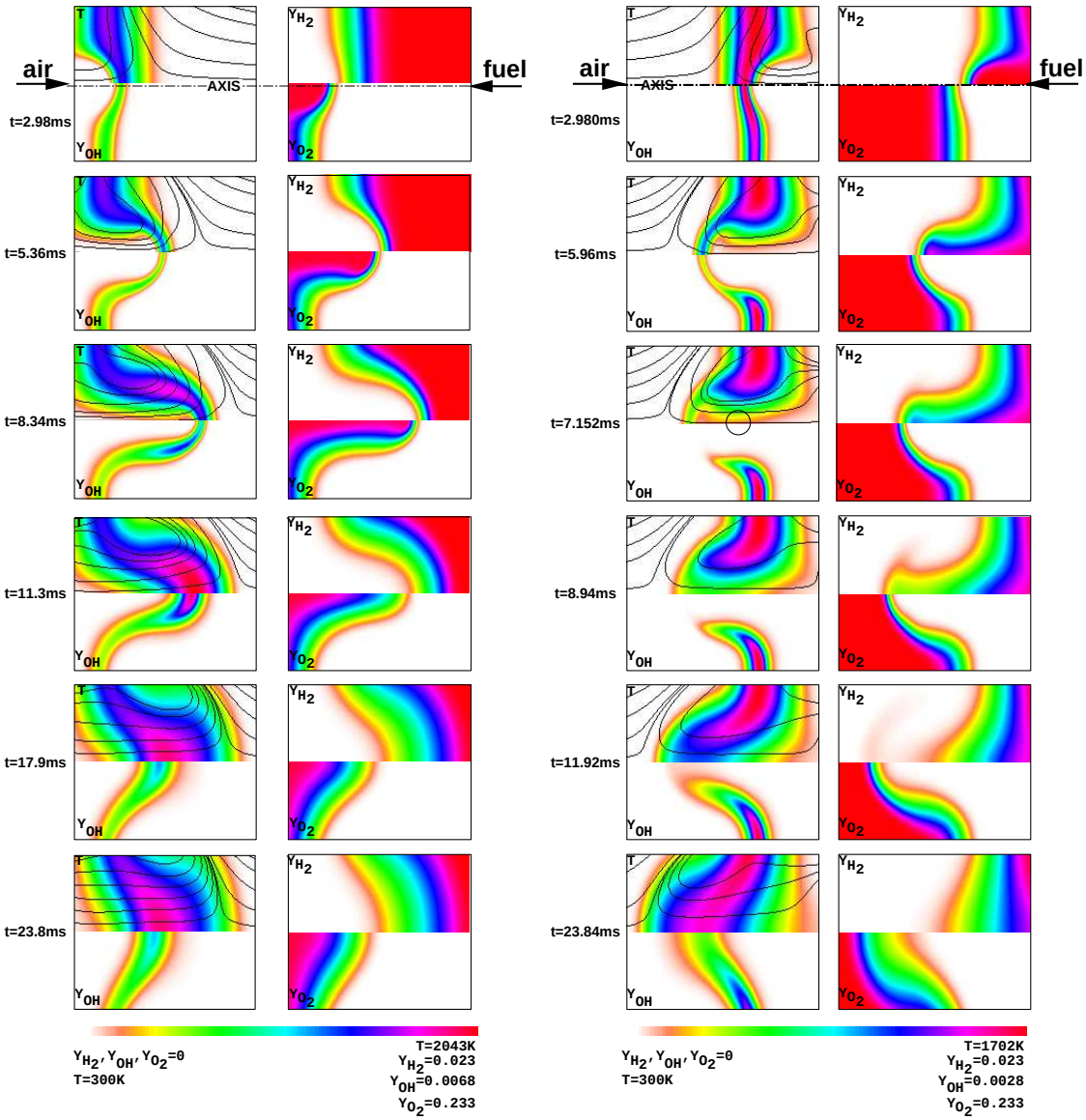

Figure 1: Time sequence of temperature and OH, H_2, O_2 mass fraction isocontours and streamlines of diffusion flame-vortex interaction in the enlarged region of the interaction. Left two columns: vortex placed on the air side of the flame. Right two columns: vortex of opposite sign placed on the fuel side of the flame. Vortex parameters: $U_{Hills} = 4.76$, $a = 0.1$

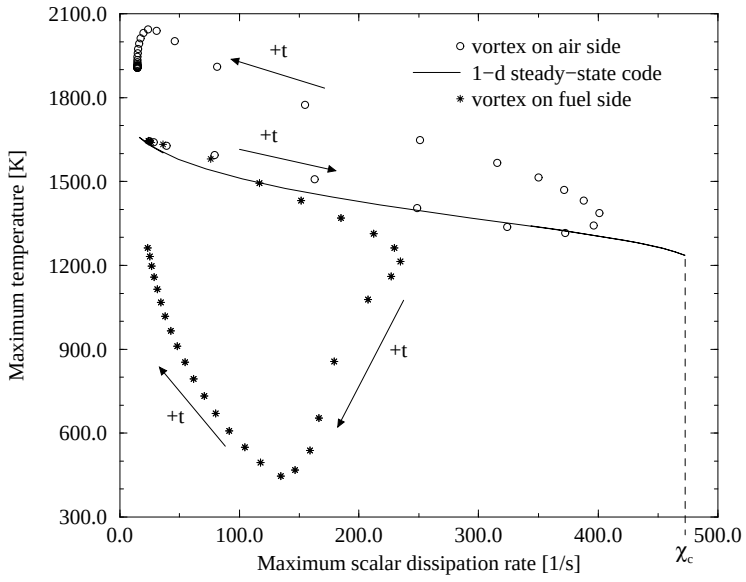

Figure 2: Comparison with a steady flamelet model. Stars: vortex placed on the fuel side, Circles: vortex placed on the air side. Solid line: response of a flat steady-state flame up until extinction. Arrows indicate increasing time.

After the formation of this edge flame, even when the applied strain rate is reduced to the initial subcritical value, the diffusion flame disc does not reappear because the local fluid velocity still exceeds the propagation speed of the edge flame. This hysteresis has significant implications for flamelet submodels that utilize the strain (or scalar dissipation) rate as a parameter to determine local reignition in turbulent combustion. It indicates that, a sub-critical strain rate may not be sufficient for the reignition (or re-establishment) of a diffusion flame.

The geometry used in the simulations is similar that of the experiment of Pellet *et al.* [8]: an axially symmetric opposed-jet burner, with fuel (40% H_2 in N_2) and air nozzles of diameter D=0.27 cm placed at a distance of L=0.27 cm apart. Cold, non-reactive walls constrain the flow and provide well-defined boundary conditions for the simulations. The numerical domain is large (the outflow boundary is placed three diameters away from the nozzles) to accommodate the edge flame which are stabilized at positions away from the axis of symmetry. The steady-state two-dimensional diffusion flame is obtained first in the two-dimensional domain at Re=508.8 (shown in the left column of Fig. 3). This diffusion flame is subjected to a near extinction scalar dissipation rate: a further increase of the Reynolds number to Re=700 extinguishes the flame in the region near the axis of symmetry. An edge flame forms and propagates radially outwards until it is stabilized at the location where its propagation speed matches the local

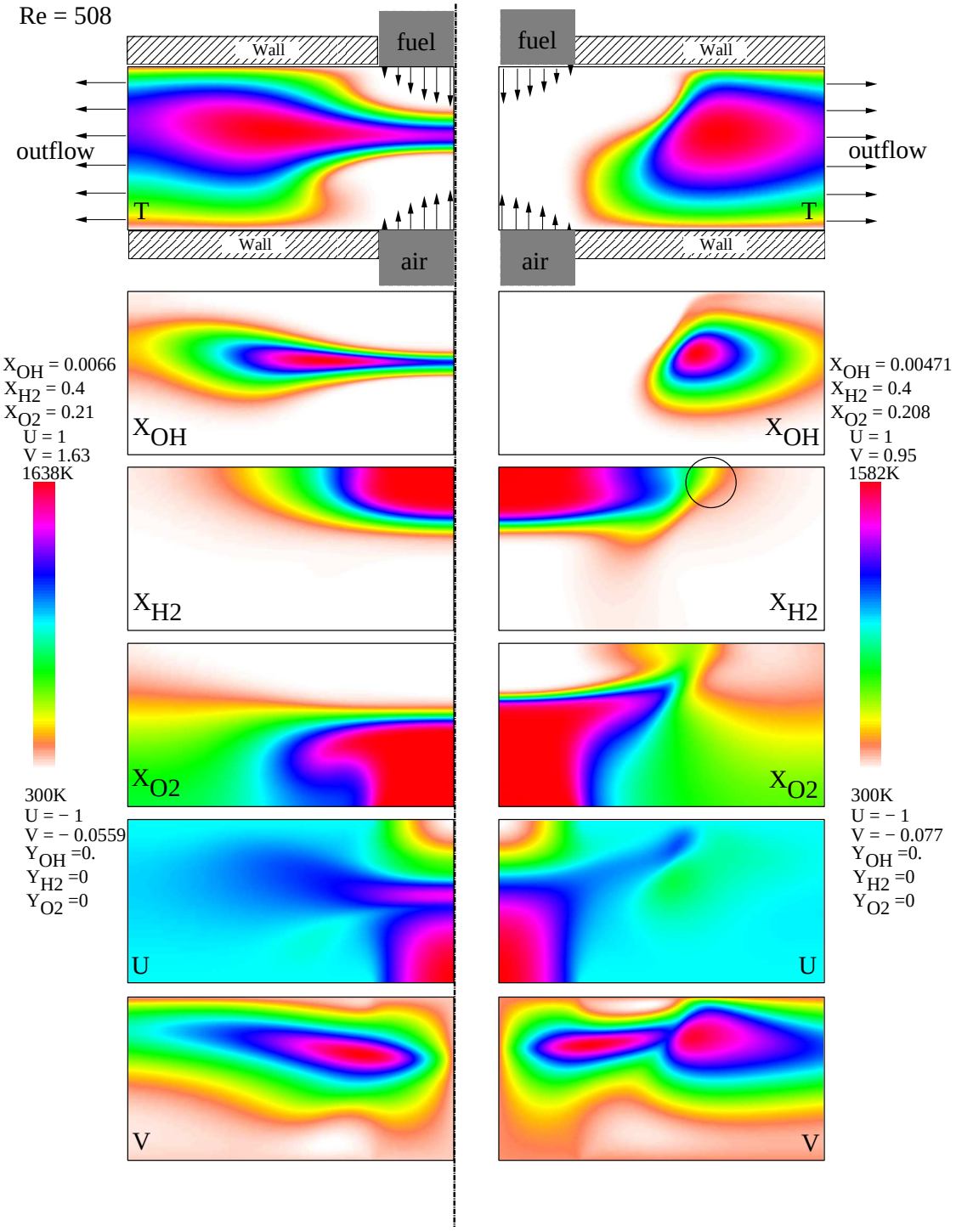

Figure 3: Isocontours of velocity components, temperature, mole fraction of selected species; left column: a contiguous diffusion flame, right column: an edge flame. Re=508.8 in both cases.

flow velocity. Starting with this stable solution (the edge flame) at Re=700, the decrease back to Re=508.8 did not lead to the re-establishment of the diffusion flame. The edge flame propagates back towards the axis but stabilizes at a finite distance from it. Isocontours of velocity components, temperature, and the mole fractions of selected species of these steady flames are depicted in Fig. 3. The left column corresponds to the diffusion flame, and the right column to the edge flame.

The simulations were then performed in the range 300≤Re≤1000. We identified the critical Reynolds number, where (a) the diffusion flame extinction near the axis of symmetry leads to an edge flame that stabilizes further away, and (b) the edge flame propagates towards the axis in the mixing layer established between the opposed-jets to re-establish the diffusion flame. The former (upper critical Re) is found to lie between 650≤Re≤675, and the latter (lower critical Re) between 318≤Re≤320. Figure 4, shows the heat release rate isocontours of the edge flames obtained at Re=320, 350, 400, 508.8, 700, and 1000 (rendered non-dimensional by $\rho_{air} c_{p,air} T_{air}$ and the corresponding convection time $t_c = D/U_{air}$). At Re=320, the diameter of the stabilized edge flame (defined as the radial location of the maximum burning rate point) is approximately equal to the radius of the inlet nozzles. At Re=318, the edge flame moves radially inwards and re-establishes the original diffusion flame. In the range $320 \leq Re \leq 1000$, steady edge flames stabilized themselves at locations where the local flow velocity normal to the flame front matches the local flame speed along the whole flame front.

Within the range of lower and upper critical Re, the two strongly-burning flames co-exist at identical conditions. Depending on the initial condition either flame type can be obtained. In addition, one can "jump" from one flame type to the other by sufficiently perturbing the corresponding flame (e.g. by locally extinguishing the diffusion flame over a large enough region, or by sufficiently heating the reacting mixture upstream of the edge flame). This means that the upper branch of the S-shaped response curve of the one-dimensional diffusion flame (corresponding to the strongly-burning diffusion flame) must be complemented by an additional branch corresponding to the edge flame. An appropriate indicator of the two flame types was the quantity $\theta = \frac{\sqrt{\mathbf{T}\cdot\mathbf{T}}}{N_p}$, where $\mathbf{T}$ is the vector containing the computed (discrete) temperature field, and N_p the total number of discretization points. In Fig. 5, θ is plotted as a function of Re: The edge flame "lives" on a new branch (open squares) and there is an extended region of Re where it coexists with the diffusion flame (the branch marked by the filled circles which corresponds to the classical upper branch of the S-shaped curve of diffusion flames). It is not yet clear how the two branches connect. The composition of the fuel stream is also expected to have a large effect on the flame structure and propagation. We are developing software that will enable both the efficient tracking of the branches, and the identification of the connecting branch.

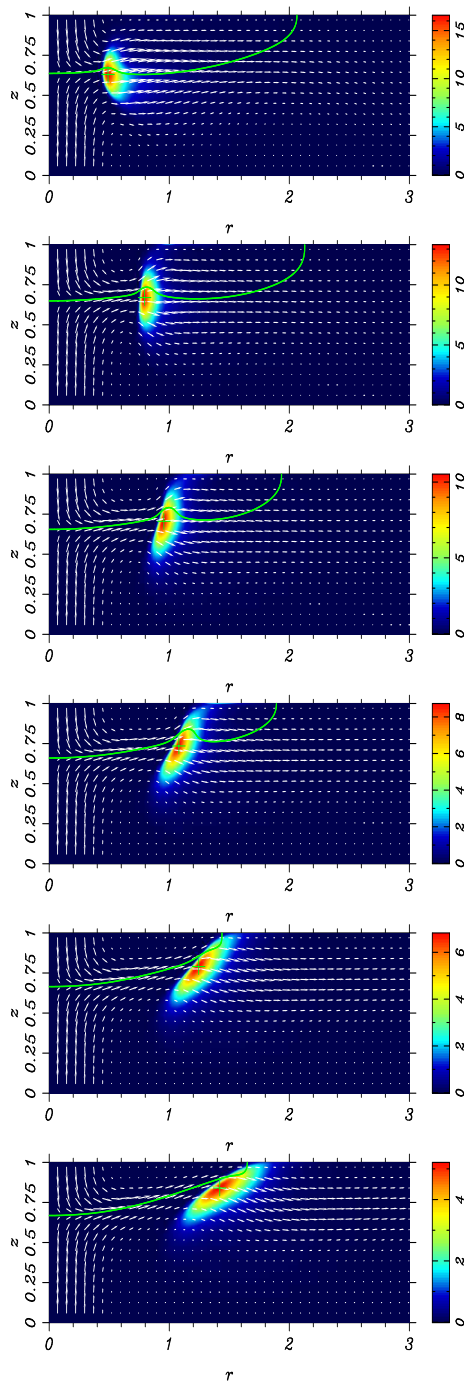

Figure 4: Non-dimensional heat release rate isocontours of the edge flames obtained at different Reynolds numbers (from top to bottom: Re=320, 350, 400, 508.8, 700, and 1000). The green dashed line indicates the stoichiometric mixture fraction and the cross is at the maximum heat release rate point.

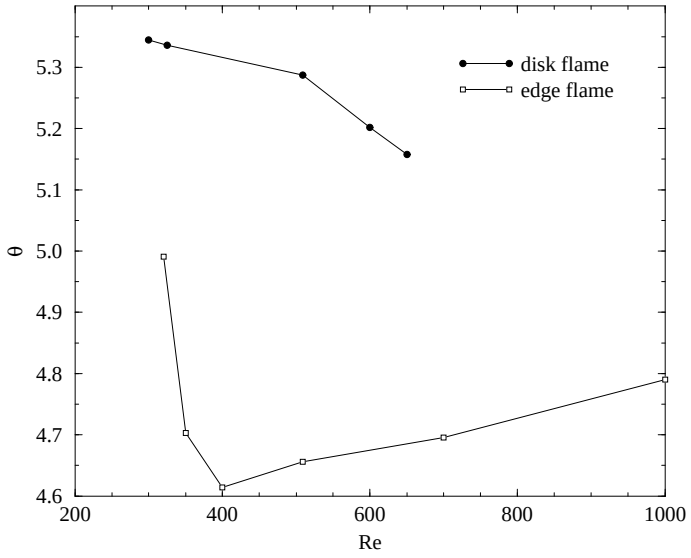

Figure 5: The two types of flames, indicated by $\theta = \frac{\sqrt{(T \cdot T)}}{N_p}$, at different Reynolds numbers. Filled circles: upper (strongly-burning) branch of the diffusion flame, open squares: edge flame

3.2.2 Transient phenomena

The time-accurate simulation results were also analyzed to study transient effects during the transitions between diffusion and edge flames. By starting from a steady flame and impulsively changing the flowrates, we simulated two different senaria: (a) extinction of diffusion flames around the axis of symmetry and formation of a propagating edge flame that ultimately leads to a ring-shaped edge flame stabilizing away from the axis of symmetry, and (b) propagation of ring-shaped premixed flames along the stoichiometric isoline through a weakly stratified mixture in the direction normal to the direction of propagation, eventually closing the flame hole and re-establishing a disk-shaped diffusion flame. Four different cases were considered: (i) the transition from the diffusion flame at Re=318 to the edge flame at Re=675 to study the "extinction" process, (ii) the reverse transition from the edge flame at Re=675 to the diffusion flame at Re=318 to study the "re-ignition" process, (iii) the transition from the edge flame at Re=400 to the diffusion flame at Re=300, and (iv) the transition from the diffusion flame at Re=650 to the edge flame at Re=675. Cases (i) and (ii) correspond to transitions over the range of co-existence, while (iii) and (iv) correspond to transitions from within (outside) to outside (within) this range. A front moving to quench or extend the diffusion flames is observed at the initial and final stages of cases (i) and (iv) and (ii) and (iii), respectively. After extinction of or before re-establishment of the diffusion tail, the flames (as a whole) move in a quasi-steady manner with

a propagating velocity relative to the fresh reactants that is close to the premixed laminar flame speed.

Figure 6 shows isocontours of the heat release rate (HRR) during the traditions in case (i) (left column) and case (ii) (right column) at different non-dimensional times. The corresponding non-dimensionalizing times are t_c=0.678 ms, and t_c=1.44 ms, respectively. As can be seen in the left column of Fig. 6, the diffusion flame is still attached to the axis of symmetry at t=1.0, whereas at t=1.5 the location of the maximum heat release rate, HRR_{max}, has already moved away from the axis. At t≈3 ms (which is close to the reciprocal of the critical scalar dissipation rate), the HRR_{max} point starts to rapidly move away from the axis. The moving edge of the diffusion flame close to the axis becomes evident at t≈5.4, while the diffusion flame gradually disappears in a process that lasts till t≈6.1. From that point on, the whole edge-flame structure moves, changes its orientation and eventually stabilizes at the location where the local flow velocity in the direction normal to the flame matches the local laminar premixed flame speed. No negatively propagating edge flame was found during extinction; before the transition to a strongly burning edge flame, the diffusion flame edge is convected outwards with the local flow velocity.

The sequence of isocontour plots (right column of Fig. 6) indicate that the edge flame moves radially inwards and eventually re-establishes the steady diffusion flame. At the early stages of the transition, the flame rapidly moves close to the nozzle edge. It stays there for a fairly long time before eventually moving towards the axis to close the flame hole. During this re-ignition process, the edge flame propagates all the way to the axis, and no homogeneous re-ignition was observed. Close to the axis it attained a propagation velocity that is almost twice the laminar flame speed.

A more detailed description of the observed phenomena can be found in the paper presented to the 29^{th} Combustion Symposium [10].

3.2.3 Methane edge flames

We are currently performing simulations for the CH_4 flame studied by Santoro *et al.* [11]. In addition to the analysis of the experimental results, the aim is to study a more complex fuel that is diffusionally balanced (Lewis number close to unity), and provide initial data for detailed experiments planned at Paul Scherrer Institute. Due to the high computational cost, a skeletal methane oxidation kinetic scheme including only the C_1 chemistry with 15 species is used. The geometry is that of an axially symmetric opposed-jet burner, with nozzles of radius 0.625 cm separated by 1.3 cm [11]. The numerical domain is extended and the outflow boundary is at a distance of 3.75 cm away from the axis to accommodate the edge flame. The geometry of the numerical domain was rectangular, with the upper and lower boundaries taken as non-reactive walls of constant temperature (300K) along which the no-slip boundary condition was enforced. These

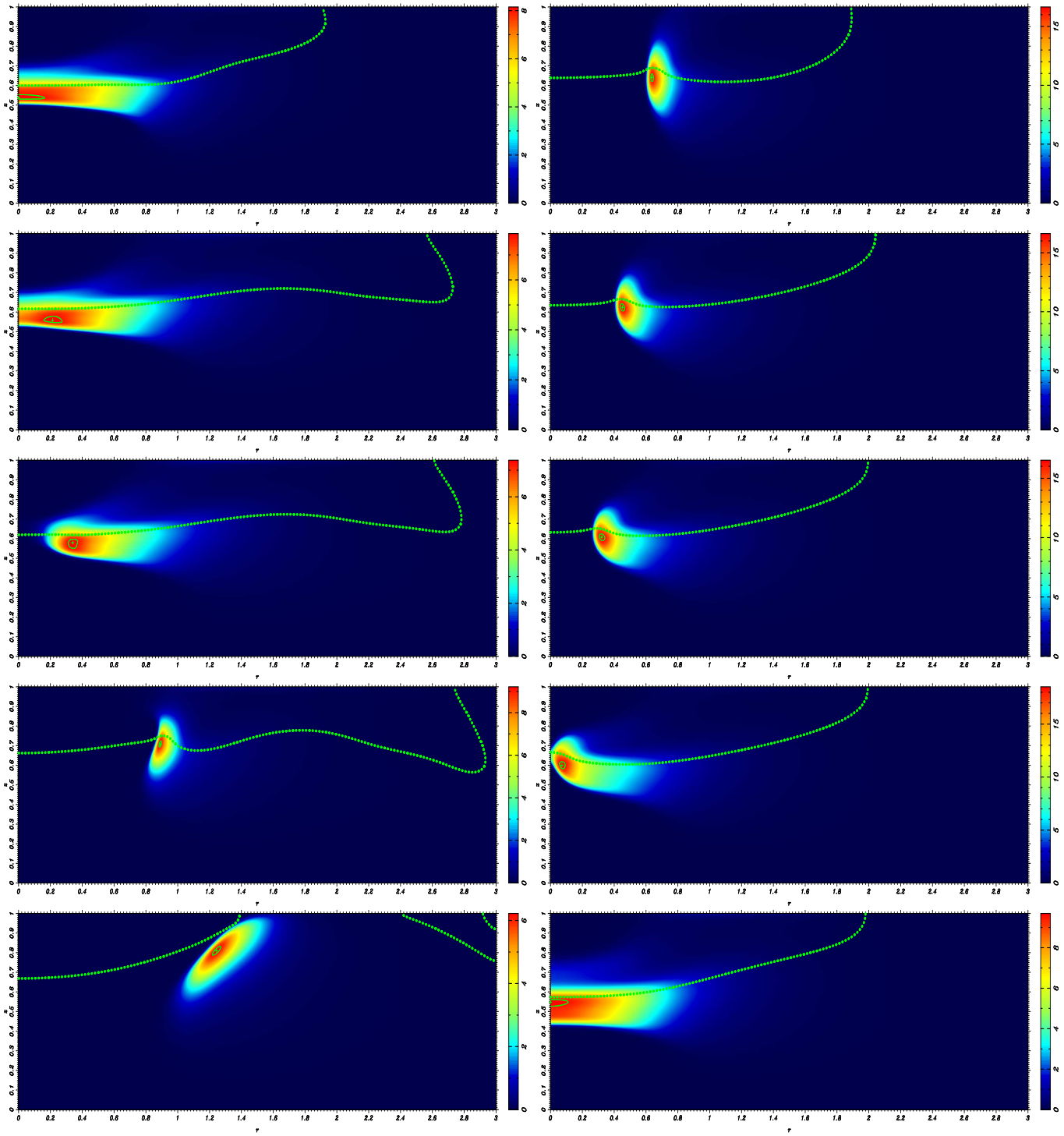

Figure 6: Isocontours HRR as a function of time for the Re=318 to Re=675 transition (left column, times from top to bottom:1, 5, 5.4, 7, 10) and the Re=675 to Re=318 (right column, times from top to bottom: 5, 15, 20, 21, 22). All quantities are non-dimensional.

wall boundary conditions is consistent with the experimental setup described in [11]; at the outflow, zero-Neumann boundary conditions is applied. The velocity profiles at the exits of the nozzles were uniform with an outflow axial velocities of 89.1 cm/s on the oxidizer nozzle and 105.8 cm/s on the fuel nozzle. Fuel was composed of 13.2% CH_4, and 86.8% N_2 (by volume at 300K), and the oxidizer of 88.6% O_2, and 11.4% N_2 (by volume at 300K).

Depicted in Fig. 7 are the instantaneous isocontours of the two components of fluid velocity, temperature, the mass fractions of CH_4, O_2, HCHO, OH, and the chemical heat release rate (HRR) at a time at which the flame propagates radially outwards with respect to a fixed frame. All quantities, with the exception of temperature (in K), are non-dimensional, and the axial and radial coordinates are denoted by z and r, respectively. The stoichiometric line is indicated by a dashed green line, and the point at which the heat release rate reaches its maximum is marked by a cross. The isocontours revealed some important features of this edge flame. Firstly, they show a highly curved flame front propagating along the stoichiometric line. However, this flame, does not exhibit a tribrachial structure, i.e. the two distinct lean and rich premixed arms, and the diffusion flame tail. The HCHO isocontours show a compressed front with significant curvature extending into the oxidizer side (as in the experiments of [11]) and a fuel rich arm that merges into a long trailing diffusion flame tail. HCO was found to be an excellent marker of the heat release rate.

3.3 Data reduction and observer construction using proper orthogonal decomposition

The numerical simulation data of the opposed-jet hydrogen/air diffusion flame were analyzed and reduced using the Proper Orthogonal Decomposition (POD) technique. Our aim was two-fold: first, to compute a small number of space-dependent empirical eigenfunctions in order to obtain a low-dimensional representation of the large original model. We found that only six modes provide an accurate representation of the system in an extended range capturing over 99% of the total "energy" of the original system with more than 26,000 degrees of freedom. This data reduction takes into account not only chemical kinetics, but also transport phenomena in a full two-dimensional context and constitutes the first step towards the construction of low-dimensional dynamic models for the opposed-jet system. Second, to use part of the available data ("measurements"), together with the computed modes, to estimate the "unmeasured" quantities. We found that only a small number of measurements are needed in order to obtain accurate estimates of the rest of the data.

Figure 8 compares the computed OH mass fraction fields with those obtained using six (left half) and nine modes (right half) and the temperature 2-D field measurement (i.e. at 101x201 points) to estimate the coefficients a_k (for the

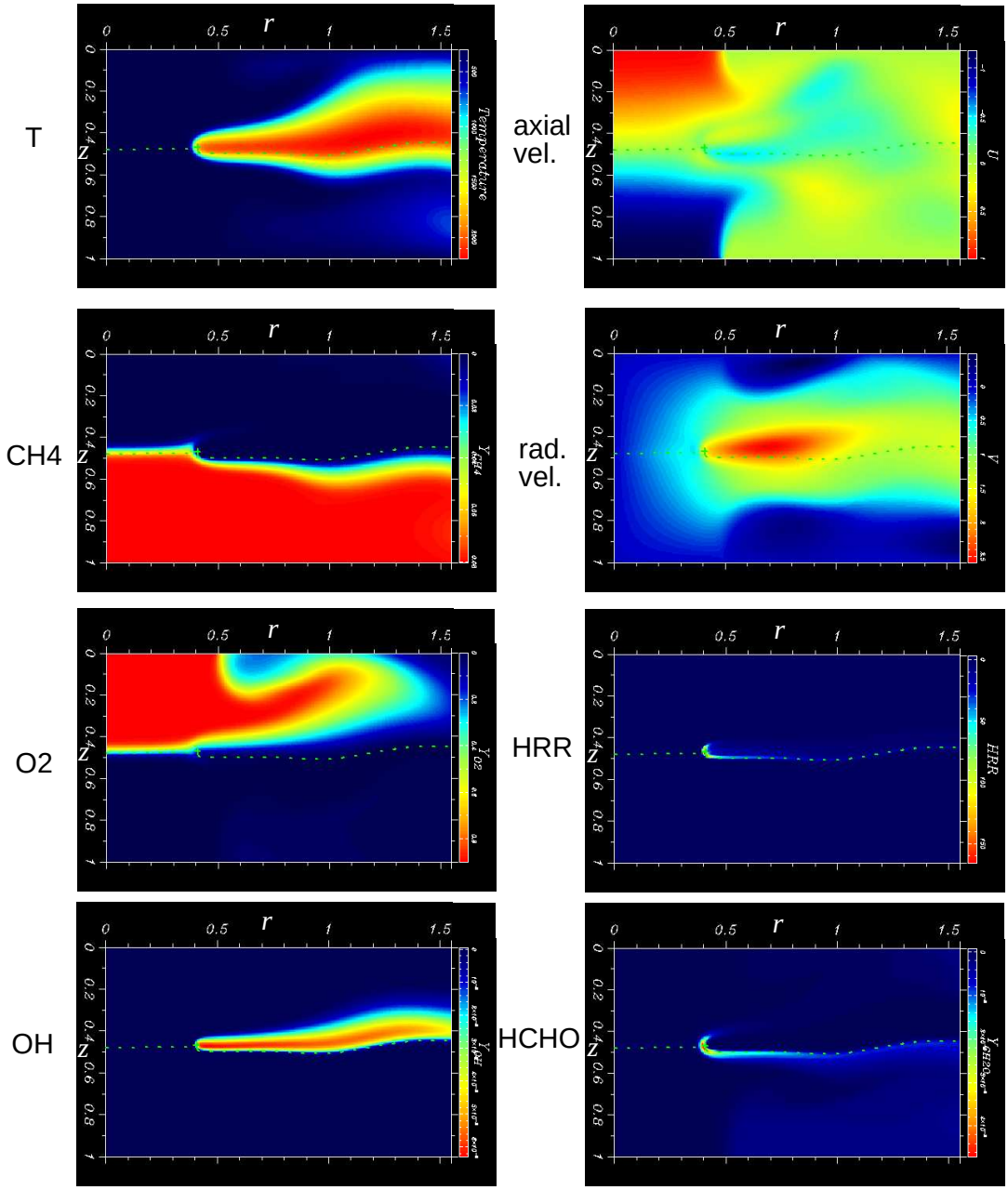

Figure 7: Isocontours of the velocity components (U,V) [non-dimensional], temperature [K], mass fraction of species (CH_4, O_2, OH, HCHO), heat release rate [non-dimensional]. The stoichiometric line is superimposed (dotted line) and the maximum heat release rate point is indicated by a cross.

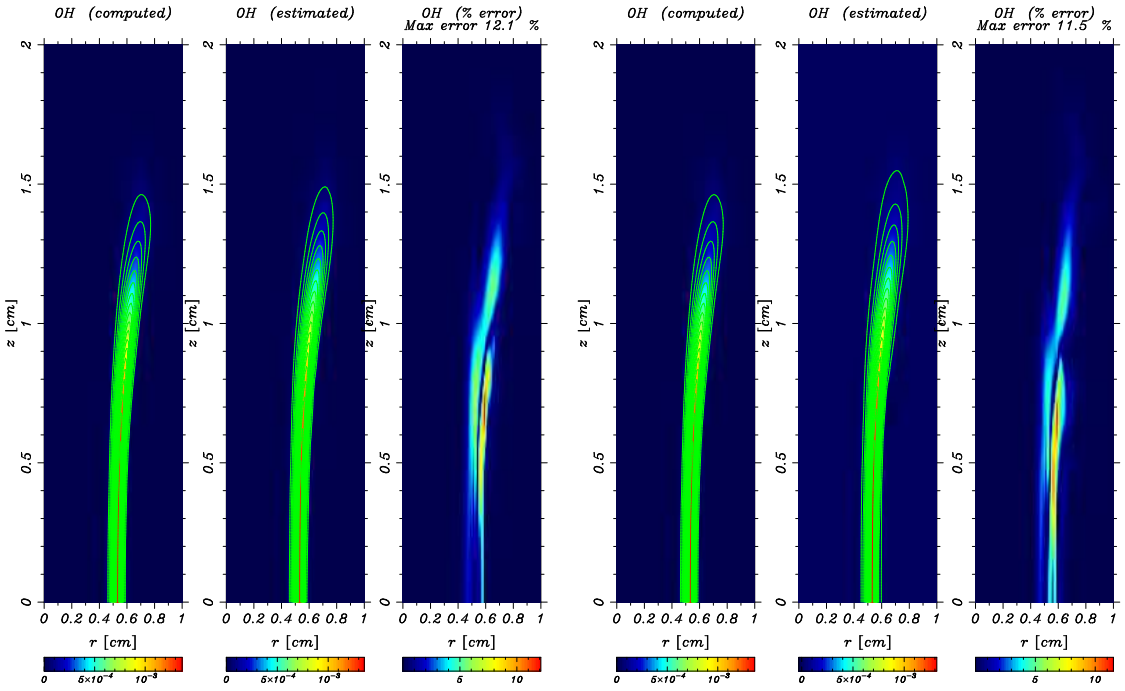

Figure 8: Comparison of the DNS OH field with its estimate using six (left) and nine (right) POD modes together with temperature 2-D measurements.

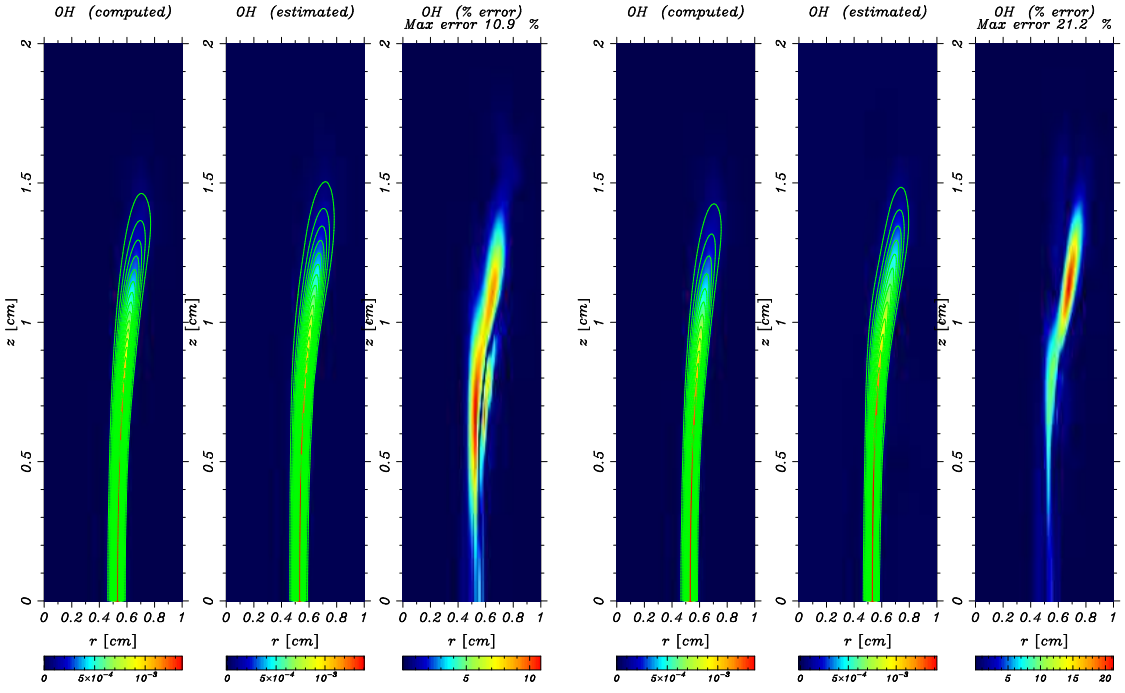

Figure 9: Comparison of the DNS OH field with its estimate using six (left) and nine (right) POD modes together with temperature measurements along the axis of symmetry.

expansion using the POD vectors) for the Re=300 case, which was not included in the data set for the computation of the POD modes, to reconstruct the data of this case. With the exception of HO_2 and H_2O_2, the "unmeasured" quantities can be estimated with less than 13% maximum relative error. Good results were obtained even when temperature is measured only at 101 points along the axis of symmetry, as shown in figure 9 for the Re=300 case. The behavior and values of the relative errors are almost unaffected. This indicates that it is indeed possible to use only a handful of carefully selected measurement points (together with the POD modes) to estimate the remaining quantities over the two-dimensional domain. More details can be found in [12].

4 Further work

The Combustion Diagnostics group of the Paul Scherrer Institute is building an opposed-jet burner for the experimental study of edge flames. We plan to compare the experimental results to our simulations and perform additional simulations for the conditions/fuels that will be used in the experiments.

We are also extending our serial 2-D DNS code to a parallel 3-D code, in collaboration with Dr. Paul Fischer of Argonne National Laboratory, USA. As a first step, implementation, testing and validation single-step chemistry is underway. Detailed chemistry and transport will be implemented in a second stage. The code is parallelized using the Message Passing Interface (MPI) and will run on the PC cluster that will be purchased at the Aerothermochemistry and Combustion Systems Laboratory. It will provide us with the means to move towards simulations of 3-D geometries as well as at higher Reynolds numbers (in the transitional or early turbulent regime).

5 Publications from this project

The work performed during this project was presented at the Combustion Symposia and other meetings and was published as follows:

- J. Lee, C. E. Frouzakis, and K. Boulouchos. Numerical study of opposed-jet H_2/air diffusion flame-vortex interactions, *Comb. Sci. Tech.*, 158:365-388, 2000.

- C. E. Frouzakis, I. Kevrekidis, Lee J., K. Boulouchos, and A. Alonso. Proper Orthogonal Decomposition of Direct Numerical Simulation data: data reduction and observer construction, In Proc. Comb. Inst., vol. 28, 2000.

- J. Lee, C. E. Frouzakis, and K. Boulouchos. Two-dimensional direct numerical simulation of opposed-jet hydrogen/air flames: Transition from a diffusion to an edge flame, In Proc. Comb. Inst., vol. 28, 2000.
- C. E. Frouzakis, A. G. Tomboulides, J. Lee, and K. Boulouchos. From diffusion to premixed flames in an H2/air opposed-jet burner: The role of edge flames, *Comb. Flame*, 130:171-184, 2002.
- C. E. Frouzakis, A. G. Tomboulides, J. Lee, and K. Boulouchos. Transient phenomena during diffusion/edge flame transitions in an opposed-jet hydrogen/air burner, In Proc. Comb. Inst., vol. 29, (in press), 2002.

These publications are appended at the end of the report.

References

[1] A. G. Tomboulides, J. C. Y. Lee, and S. A. Orszag. Numerical simulation of low mach number reactive flows. *J. Sci. Comp.*, 12(2):139–167, 1997.

[2] A. G. Tomboulides and S. A. Orszag. A quasi two-dimensional benchmark problem for low Mach number compressible codes. *J. Comp. Phys.*, 146(2):691–706, 1998.

[3] P. N. Brown, G. D. Byrne, and A. C. Hindmarsh. VODEPK: A Variable Coefficient ODE Solver. *SIAM J. Sci. Stat. Comput.*, 10(5):1038–1051, 1989.

[4] J. Lee, C. E. Frouzakis, and K. Boulouchos. Numerical study of opposed-jet H_2/air diffusion flame-vortex interactions. *Comb. Sci. Tech.*, 158:365–388, 2000.

[5] C. E. Frouzakis, A. G. Tomboulides, J. Lee, and K. Boulouchos. From diffusion to premixed flames in an H_2/air opposed-jet burner: The role of edge flames. *Comb. Flame*, 130:171–184, 2002.

[6] N Peters. Laminar flamelet concepts in turbulent combustion. *Proc. Comb. Inst.*, 21:1231, 1986.

[7] A. E. Potter and J. N. Butler. A novel combustion measurement based on the extinguishment of diffusion flames. *ARS J.*, 29:54:54–56, 1959.

[8] G. L. Pellet, K. M. Isaac, W. M. Jr. Humphreys, L. R . Gartrell, W. L. Roberts, C. L. Dancey, and G. B. Northam. Velocity and thermal structure, and strain-induced extinction of 14 to 100% hydrogen-air counterflow diffusion flames. *Combust. Flame*, 112:575–592, 1998.

[9] J. Lee, C. E. Frouzakis, and K. Boulouchos. Two-dimensional direct numerical simulation of opposed-jet hydrogen/air flames: Transition from a diffusion to an edge flame. In *Proc. Comb. Inst.*, volume 28, pages 801–806, 2000.

[10] C. E. Frouzakis, Tomboulides A. G., Lee J., and K. Boulouchos. Transient phenomena during diffusion/edge flame transitions in an opposed-jet hydrogen/air burner. In *Proc. Comb. Inst., (in press)*, volume 29, 2002.

[11] V. S. Santoro, A. Liñán, and A. Gomez. Propagation of Edge Flames in Counterflow Mixing Layers: Experiments and Theory. In *Proc. Comb. Inst.*, volume 28, pages 2039–2046, 2000.

[12] Frouzakis C. E., Kevrekidis I., Lee J., K. Boulouchos, and Alonso A. Proper orthogonal decomposition of direct numerical simulation data: data reduction and observer construction. In *Proc. Comb. Inst.*, volume 28, 2000.